자원환경지질, 제44권, 제2호, 161-170, 2011
Econ. Environ. Geol., 44(2), 161-170, 2011

# Development of Multiphase Flow Simulator Using the Fractional Flow Based Approach for Wettability Dependent NAPL Migration

**Heejun Suk[1]*, In Wook Yeo[2] and Kang Kun Lee[3]**

[1]*Geologic Environment Division, Korea Institute of Geosciences and Mineral Resources*
[2]*Department of Earth and Environmental Sciences, Chonnam National University*
[3]*School of Earth and Environmental Sciences, Seoul National University*

# 친수성에 의존하는 소수성 액체의 거동을 위한 분율 유동 접근 방식을 이용한 다상 유동 수치 모델링 개발

**석희준[1]* · 여인욱[2] · 이강근[3]**

[1]한국지질자원연구원, [2]전남대학교 지구환경과학과, [3]서울대학교 지구환경과학부

석유공학분야에서 보고된 분율 흐름 접근 방식을 이용하여 물리적 또는 화학적으로 불균질한 매질에서 완전한 삼상유체를 고려할 수 있는 다상 흐름 수치 모의 프로그램인 CHEMPS가 개발되었다. 이 프로그램은 석희준과 G.T. Yeh (2008)에 의해 개발된 MPS을 확장하였는데, 친수성이 NAPL 거동에 미치는 영향을 모의하기 위하여 개발되었다. 대부분 존재하는 모델들은 물리적으로 불균질한 매질을 고려하고 이상흐름과 특정한 경계조건에 국한되어 있다. 게다가 대부분의 모델들은 주로 water-wet 매질에만 국한되어 있다. 그러나 실제 존재하는 시스템에서는, water-wet과 oil-wet 매질 사이의 친수성의 변화는 종종 일어난다. 더군다나 기름에 의한 다공성 매질의 젖음은 균등하기 보다는 불균질 또는 부분적일 수 있다. 왜냐하면 친수성에 영향을 미치는 요소들과 지하 매질이 불균질하기 때문이다. 따라서, 이번 연구에서는 물리적으로 불균질한 매질 뿐만 아니라 친수성 면에서 화학적으로 불균질한 매질을 CHEMPS을 활용하여 수치모의 하였다. 그 외에도 개개의 상에 대해서 유량 경계조건 및 고정경계조건의 두 가지 형식의 결합으로 표현되는 일반경계조건이 고려되었다.

**주요어** : 다중상 흐름, 분율 흐름 접근, 물리적 및 화학적으로 불균질한 매질

The multiphase flow simulator, CHEMPS, was developed based on the fractional flow approach reported in the petroleum engineering literature considering fully three phase flow in physically and chemically heterogeneous media. It is a extension of MPS developed by Suk and Yeh (2008) to include the effect of wettability on the migration of NAPL. The fractional flow approach employs water, total liquid saturation and total pressure as the primary variables. Most existing models are limited to two-phase flow and specific boundary conditions when considering physically heterogeneous media. In addition, these models focused mainly on the water-wet media. However, in a real system, variations in wettability between water-wet and oil-wet media often occur. Furthermore, the wetting of porous media by oil can be heterogeneous, or fractional, rather than uniform due to the heterogeneous nature of the subsurface media and the factors that affect the wettability. Therefore, in this study, the chemically heterogeneous media considering fractional wettability as well as physically heterogeneous media were simulated using CHEMPS. In addition, the general boundary conditions were considered to be a combination of two types of boundaries of individual phases, flux-type and Dirichlet type boundaries.

**Key words** : multiple phase flow, fractional flow approach, physically and chemically heterogeneous media

## 1. Introduction

Two main approaches have been developed for modeling multi-phase flow that arises in hydrology and petroleum engineering. The first is based on individual balance equations for each of the fluids,

*Corresponding author: sxh60@kigam.re.kr

while the second involves the manipulation and combination of those balance equations into modified forms, with the concomitant introduction of ancillary functions, such as the fractional flow function. The first approach is referred to as pressure-based, while the second approach is referred to as fractional flow-based. The pressure approach is used widely in the hydrology literature. In this approach, the governing equations are written in terms of the pressures through a straightforward substitution of Darcy's equation into the mass balance equations for each phase. This approach was adopted by a number of authors, (Pinder and Abriola, 1986; Sleep and Sykes, 1989; Kaluarachchi and Parker, 1989; Celia and Binning, 1992; Kueper and Frind, 1991a, b; Bastian and Helmig, 1999; Dekker and Abriola, 2000; Bradford *et al.*, 1998). The fractional flow approach reported in the petroleum engineering literature employs water saturation, total liquid saturation, and a total pressure as the primary and independent variables. This approach leads to three equations: one pressure and two saturation equations. The fractional approach has been employed by many authors (Guarnaccia and Pinder, 1997; Binning and Celia, 1999; Suk and Yeh, 2008). However, until now, most fractional flow approaches have been limited to two-phases and specific boundary conditions in only physically heterogeneous media. Usually, boundary conditions are the Dirichlet-type, which is impractical for real problems because it is impossible to know the pressure of infiltrating phases over time. In addition, most numerical studies have assumed that the porous media were strongly water-wet, and employed limiting assumptions that the intermediate wetting fluid (oil) forms a continuous layer between the wetting (water) and nonwetting (air) fluids (Suk and Yeh, 2008). However, a real system does not follow this assumption. Therefore, the capillary behavior has great sensitivity to multiphase flow, suggesting that large errors might be introduced into numerical simulations when the water-wet assumption does not hold (Bradford *et al.*, 1998). Bradford and Leij (1996) developed a capillary pressure and saturation relationship that can consider even a discontinuous layer between wetting and non-wetting phases.

In this paper, a two-dimensional finite element model (CHEMPS – **CHE**mical and physical **M**ulti**P**hase **S**imulator) was developed to examine the simultaneous movement of nonaqueous phase liquid, water and gas in physically and chemically heterogeneous porous media. Here, the physically heterogeneous media is characterized mainly by the intrinsic permeability and van Genuchten parameter reflecting the pore size distribution, while chemically heterogeneous media was characterized using the empirical relations developed by Bradford and Leij (1996) and Bradford *et al.* (1997, 1998). CHEMPS included the general boundary condition consisting of eight combinations of two types of boundaries of individual phases, the flux-type and Dirichlet-type boundaries, as well as the general initial conditions comprised of eight combinations of two types of the initial condition of individual phases, saturation and pressure. Therefore, regardless of the type of initial and boundary conditions specified among the eight types, they can be transformed and incorporated into manageable initial and boundary conditions. A pressure equation was solved to obtain the total pressure distribution using the standard Galerkin finite element method. The total velocity distribution was determined using the calculated total pressure distribution. The upstream finite element method was employed to solve the two saturation equations. In order to obtain a simultaneous solution of saturation equations, various solvers, such as the Bi-CGSTAB (van der Vorst, 1992) method, modified incomplete Cholesky method (MICPCG), direct Gaussian elimination method, and pointwise iterative solver (PISS), were used. A distinctive feature is that phase flow equations are given in a fractional flow formulation, i.e., in terms of water saturation, total liquid saturation and total pressure. In addition, CHEMPS can handle the three phases flow problem in chemically heterogeneous and physically heterogeneous media. Furthermore, this does not need to specify a small, fictitious degree of nonwetting saturation, where only the wetting phase is present, as is normally required with more traditional pressure-based simulators, because these variables exist throughout the solution domain regardless of whether the non-wetting phase is present (Kaluarachchi and Parker, 1989). The two verifications and three application examples was provided.

## 2. Governing Equations

A multiphase system in porous media was assumed to be composed of three phases: NAPL, gas and water. Each of the three phases was treated with the averaged properties of the fluid, even though each of the three phases might contain several components. The case of incompressible fluids was considered for simplicity. The equations for the flow of three fluid phases in a porous medium are given by the conservation of mass ($\alpha = 1$ for water, 2 for NAPL, and 3 for gas)

$$\frac{\partial(\phi\rho_\alpha S_\alpha)}{\partial t}+\nabla\bullet\rho_\alpha V_\alpha=0 \tag{1}$$

and the Darcy velocity of phase $\alpha$, $V_\alpha$, is defined as

$$V_\alpha=-\frac{k_{r\alpha}\mathbf{k}}{\mu_\alpha}(\nabla P_\alpha-\rho_\alpha g\nabla z) \tag{2}$$

where $\phi$ is the effective porosity of the porous medium, $\rho_\alpha$ is the density of phase $\alpha$, $S_\alpha$ is the saturation of phase $\alpha$, $\mathbf{k}$ is the intrinsic permeability tensor, $k_{ra}$ is the relative permeability of phase $\alpha$, $\mu_\alpha$ is the dynamic viscosity of phase $\alpha$, $P_\alpha$ is the pressure of phase $\alpha$, g is the gravitational constant, and z is the depth. For the three phases case, the total velocity, $\vec{V}_t$, which is defined as the sum of the phase velocities, is given as

$$\begin{aligned}\vec{V}_t &= \vec{V}_1+\vec{V}_2+\vec{V}_3\\ &=-\frac{k_{r1}\mathbf{k}}{\mu_1}(\nabla P_1-\rho_1 g\nabla z)-\frac{k_{r2}\mathbf{k}}{\mu_2}(\nabla P_2-\rho_2 g\nabla z)\\ &\quad-\frac{k_{r3}\mathbf{k}}{\mu_3}(\nabla P_3-\rho_3 g\nabla z)\end{aligned} \tag{3}$$

where $\vec{V}_1$, $\vec{V}_2$ and $\vec{V}_3$ are water, NAPL and gas phase velocities. If Equation (3) is manipulated by defining the total mobility, $\kappa=\mathbf{k}(k_{r1}/\mu_1+k_{r2}/\mu_2+k_{r3}/\mu_3)$, and fractional mobility for phase i, $\kappa_i=k_{ri}/\mu_i/\sum_{j=1}^{3}k_{rj}/\mu_j$, for i=1, 2, and 3, Equation (4) can be obtained as follows:

$$\begin{aligned}\vec{V}_t=&-\kappa\left[\left(\frac{\kappa_1+\kappa_2+\kappa_3}{3}\right)\nabla(P_1+P_2+P_3)\right]\\ &-\kappa\left[\left(\frac{\kappa_1-\kappa_2}{2}\right)\nabla(P_1-P_2)+\left(\frac{\kappa_1-\kappa_3}{2}\right)\nabla(P_1-P_3)\right.\\ &\left.+\left(\frac{\kappa_2-\kappa_3}{2}\right)\nabla(P_2-P_3)\right]-\kappa\bar{\rho}g\nabla z\end{aligned} \tag{4}$$

where $\bar{\rho}=\kappa_1\rho_1+\kappa_2\rho_2+\kappa_3\rho_3$ is the mobility weighted average fluid density.

Since $\kappa_1+\kappa_2+\kappa_3=1$, Equation (4) becomes

$$\begin{aligned}\vec{V}_t=&-\kappa\left[\frac{1}{3}\nabla(P_1+P_2+P_3)\right]\\ &-\kappa\left[\left(\frac{\kappa_1-\kappa_2}{3}\right)\nabla(P_1-P_2)+\left(\frac{\kappa_1-\kappa_3}{3}\right)\nabla(P_1-P_3)\right.\\ &\left.+\left(\frac{\kappa_2-\kappa_3}{3}\right)\nabla(P_2-P_3)\right]-\kappa\bar{\rho}g\nabla z\end{aligned} \tag{5}$$

If the total pressure, $P_t$, is defined as

$$\begin{aligned}P_t=&\frac{P_1+P_2+P_3}{3}\\ &+\frac{1}{3}\left(\int_0^{P_1-P_2}(\kappa_1-\kappa_2)d\eta+\int_0^{P_1-P_3}(\kappa_1-\kappa_3)d\eta+\int_0^{P_2-P_3}(\kappa_2-\kappa_3)d\eta\right)\end{aligned} \tag{6}$$

Equation (5) becomes

$$\vec{V}_t=-\kappa[\nabla P_t+\bar{\rho}g\nabla z] \tag{7}$$

Therefore, the pressure equation is obtained as follows:

$$-\nabla\bullet\kappa(\nabla P_t+\bar{\rho}g\nabla z)=0 \tag{8}$$

The following equations relating the individual phase flux, $\vec{V}_1$, $\vec{V}_2$, and $\vec{V}_3$ to the total flux $\vec{V}_t$ were derived through the algebraic manipulation of Equation (2):

$$\vec{V}_1=\kappa_1\vec{V}_t-\kappa_1\kappa(\kappa_2\nabla P_{C12}+\kappa_3\nabla P_{C13})-\kappa_1\kappa(\rho_1 g\nabla z-\bar{\rho}\,g\nabla z) \tag{9}$$

$$\vec{V}_2=\kappa_2\vec{V}_t-\kappa_2\kappa(\kappa_1\nabla P_{C21}+\kappa_3\nabla P_{C23})-\kappa_2\kappa(\rho_2 g\nabla z-\bar{\rho}\,g\nabla z) \tag{10}$$

$$\vec{V}_3=\kappa_3\vec{V}_t-\kappa_3\kappa(\kappa_1\nabla P_{C31}+\kappa_2\nabla P_{C32})-\kappa_3\kappa(\rho_3 g\nabla z-\bar{\rho}\,g\nabla z) \tag{11}$$

where $P_{C12}$ ($P_{C21}$) is the capillary pressure of water (NAPL) and NAPL (water), $P_{C13}$ ($P_{C31}$) is the capillary pressure of water (gas) and gas (water), $P_{C23}$ ($P_{C32}$) is the capillary pressure of NAPL (gas) and gas (NAPL). Substitution of Equation (9) and (11) into (1), and assuming incompressible flow and the continuity of total flux results in the following two saturation equations, respectively:

$$\frac{\partial \phi S_l}{\partial t}+\vec{V}_l \bullet \frac{d\kappa_1}{dS_1}\nabla S_1=\nabla \bullet \kappa_1 \kappa\left(\kappa_2 \frac{\partial P_{C12}}{\partial S_1}+\kappa_3 \frac{\partial P_{C13}}{\partial S_1}\right)\nabla S_1 +\nabla \bullet \kappa_1 \kappa\left(\kappa_2 \frac{\partial P_{C12}}{\partial S_t}+\kappa_3 \frac{\partial P_{C13}}{\partial S_t}\right)\nabla S_t+\nabla \bullet \kappa_1 \kappa(\rho_1-\bar{\rho})g\nabla z \tag{12}$$

$$-\frac{\partial \phi S_t}{\partial t}+\vec{V}_t \bullet \frac{d\kappa_3}{dS_t}\nabla S_t=\nabla \bullet \kappa_3 \kappa\left(\kappa_2 \frac{\partial P_{C32}}{\partial S_1}+\kappa_1 \frac{\partial P_{C31}}{\partial S_1}\right)\nabla S_1 +\nabla \bullet \kappa_3 \kappa\left(\kappa_2 \frac{\partial P_{C32}}{\partial S_t}+\kappa_1 \frac{\partial P_{C31}}{\partial S_t}\right)\nabla S_t+\nabla \bullet \kappa_3 \kappa(\rho_3-\bar{\rho})g\nabla z \tag{13}$$

where $S_t=S_1+S_2$ is the total liquid saturation. The set of partial differential equations given by Equations (12) and (13) were coupled through several constitutive relationships which will be discussed below. The following relationship will be needed to complete the description of multiphase flow through porous media.

$$S_1+S_2+S_3=1 \tag{14}$$

Here, the capillary pressure and saturation relationship incorporating the influence of wettability followed the model developed by Bradford and Leij (1996) and Bradford *et al.* (1998). When the contact angle was independent of saturation, the wettability effects on the capillary pressure and saturation relations were obtained by scaling the perfectly wetted capillary pressure and saturation relationships.

$$P_C^*(S)=\cos(\theta)P_C(S) \tag{15}$$

where $P_C^*$ denotes the wettability dependent capillary pressure, $P_C$ is the capillary pressure for water perfectly wet systems, and $\theta$ is the contact angle. For saturation dependent wettability, the shifted capillary pressure and saturation relationships are as follows (Bradford and Leij, 1996; Bradford *et al.*, 1998).

$$P_{C21}^*(S_1,F_0)=\frac{\rho_1 g}{\alpha_{21}}\left[S_1^{-1/m_{21}}-1\right]^{1/n_{21}}-\frac{\rho_1 g \sigma_{21} R^{ref}(0.5)}{\sigma_{21}^{ref} R(0.5)}\lambda(F_0) \tag{16}$$

$$P_{C32}^*\left(S_{t(2)}\right)=\frac{\rho_1 g}{\alpha_{32}}\left[S_{t(2)}^{-1/m_{32}}-1\right]^{1/n_{32}} \tag{17}$$

$$P_{C32}^*\left(S_{t(1)},S_2,F_0\right)=\frac{\rho_1 g}{\alpha_{32}}\left[S_2^{-1/m_{32}}-1\right]^{1/n_{32}}+\rho_1 g A(F_0)\left[S_{t(1)}-S_2\right] \tag{18}$$

$$P_{C31}^*\left(S_{t(2)},S_1,F_0\right)=P_{C21}^*\left(S_1,F_0\right)+P_{C32}^*\left(S_{t(2)}\right) \tag{19}$$

$$P_{C31}^*\left(S_{t(1)},S_2,F_0\right)=P_{C21}^*\left(S_1,F_0\right)+P_{C32}^*\left(S_{t(1)},S_2,F_0\right) \tag{20}$$

where $\lambda$ is the shifting parameter that depends on $F_0$, which indicates the organic wet mass fraction; $\alpha_{21}$, $n_{21}$, and $m_{21}$ are the van Genuchten parameters obtained by fitting the capillary pressure model of van Genuchten (1980) to the two phase capillary pressure data between NAPL and water, whereas $\alpha_{32}$, $n_{32}$, and $m_{32}$ are the van Genuchten parameters obtained by fitting the capillary pressure model of van Genuchten to the two phase capillary pressure data between air and NAPL; $\sigma_{21}^{ref}$ and $\sigma_{21}$ are the interfacial tension between water and NAPL of the reference system and other fluid systems, respectively; $R^{ref}(0.5)$ and $R(0.5)$ are the pore radius that empties at water saturation equal to 0.5 in the reference system and other porous systems, respectively; $S_{t(1)}$ is the total liquid saturation when water saturation is changed at constant NAPL saturation; $S_{t(2)}$ is the total liquid saturation when NAPL saturation is changed at constant water saturation; and $A$ is the fitting parameter meaning the slope of the capillary pressure between air and the NAPL relationship in Equation (18). In this case, $\lambda$ and $A$ was defined as

$$\lambda(F_0)=0.1135\times F_0+1.81 \tag{21}$$

$$A(F_0)=0.068\times F_0-7.52 \tag{22}$$

The effects of a change in wettability on the relative permeability relations were modeled using the modified Mualem model according to the approach presented by Bradford *et al.* (1997), who employed the modified Burdine model. It was assumed that NAPL and water will be found in the small and medium pore domains, and that air is restricted to the largest pore domain because air is always a non-wetting fluid.

$$k_{r1}(S_1,S_2)=(S_1)^{\frac{1}{2}}\frac{[1-f(\theta)]\left[\int_0^{S_1}R(x)dx\right]^2+f(\theta)\left[\int_{S_2}^{S_t}R(x)dx\right]^2}{\left[\int_0^1 R(x)dx\right]^2} \quad (23)$$

where $f(\theta)$ is an empirical weighting function that depends on the macroscopic contact angle of the medium, in which the contact angle can be estimated from $\theta=\cos^{-1}(P_C^*/P_C)$ according to scaling arguments; R is the radius of the capillary tube; and the limits of integration of the first and second integrals in the numerator assign water to the small and medium pore domains, respectively. Based on the available experimental evidence, the following functional form of the empirical weighting function was suggested by Bradford *et al.* (1997, 1998),

$$f(\theta)=\frac{1}{2}[1-\cos(\theta)] \quad (24)$$

Similarly, the relative permeability of NAPL considering the effect of the wettability is defined as

$$k_{r2}(S_1,S_2)=(S_2)^{\frac{1}{2}}\frac{f(\theta)\left[\int_0^{S_2}R(x)dx\right]^2+[1-f(\theta)]\left[\int_{S_1}^{S_t}R(x)dx\right]^2}{\left[\int_0^1 R(x)dx\right]^2} \quad (25)$$

The value of $k_{r3}$ was equal to the air relative permeability in a perfectly water wet system.

$$k_{r3}(S_t)=(1-S_t)^{\frac{1}{2}}\frac{\left[\int_{S_t}^1 R(x)dx\right]^2}{\left[\int_0^1 R(x)dx\right]^2} \quad (26)$$

### 2.1. Initial and Boundary Conditions

When Equations (8), (12) and (13) are supplemented with the appropriate boundary conditions, they can be solved for the unknowns, $P_t$, $S_1$ and $S_t$. The initial boundary conditions could be expressed as combinations of the pressure and saturation of each phase as follows:

$$P_i=P_i(x,z) \text{ on } \Omega \text{ for i=1, 2, and 3} \quad (27)$$

or

$$S_i=S_i(x,z) \text{ on } \Omega \text{ for i=1, 2, and 3} \quad (28)$$

where $\Omega$ indicates the entire simulation domain. Table 1 lists eight types of initial conditions. Regardless of which type of initial condition is specified, they must be transformed into the following three primary variables, $S_1$, $S_t$, and $P_t$. The transformation was straightforward using Equations (6), and (16) to (20).

**Table 1.** Eight types of initial conditions for the multiphase flow simulation

| Types | $P_1$ | $P_2$ | $P_3$ | $S_1$ | $S_2$ | $S_3$ |
|---|---|---|---|---|---|---|
| 1 | × | × | × | | | |
| 2 | × | × | | | | × |
| 3 | × | | × | | × | |
| 4 | | × | × | × | | |
| 5 | | | × | × | × | |
| 6 | | × | | × | | × |
| 7 | × | | | | × | × |
| 8 | | | | × | × | × |

**Table 2.** Eight types of boundary condition for the multiphase flow simulation

| Types | $P_1$ | $P_2$ | $P_3$ | $\vec{n}\bullet\vec{V}_1$ | $\vec{n}\bullet\vec{V}_2$ | $\vec{n}\bullet\vec{V}_3$ |
|---|---|---|---|---|---|---|
| 1 | | | | × | × | × |
| 2 | | | × | × | × | |
| 3 | | × | | × | | × |
| 4 | × | | | | × | × |
| 5 | × | × | × | | | |
| 6 | × | × | | | | × |
| 7 | × | | × | | × | |
| 8 | | × | × | × | | |

The boundary conditions can be written as a combination of two types of boundaries of individual phases, flux-type and Dirichlet type boundaries.

$$P_i=P_{ni}(x_b,z_b,t) \text{ on } B_{di} \quad (29)$$

$$\vec{V}_t\bullet\vec{n}=q_{ni}(x_b,z_b,t) \text{ on } B_{fi} \quad (30)$$

where $(x_b,z_b)$ is the spatial coordinate on the boundary, $\vec{n}$ is the outward unit vector normal to the boundary, $P_{ni}$ and $q_{ni}$ are the prescribed Dirichlet functional value and flux value of phase i, respectively, $B_{di}$ and $B_{fi}$ are the Dirichlet and flux boundaries for the $i^{th}$ phase, respectively. Table 2 lists the eight types of boundary conditions. Similarly to the initial condition, regardless of which type of boundary condition is specified, they can be incorporated into the boundary condition in terms of water and air phase variables because the primary variables are water and total liquid saturation, which is equal to one minus the air saturation. However, because the boundary values of all types excluding types 1

and 5 were not specified explicitly in terms of the water and air phase variables, these boundary values should be estimated from the capillary pressure relationship and Equations (9), (10) and (11) relating the individual phase flux to the total flux, and need to be iterated until the three primary variables are constant within the specified error tolerance during the iteration.

## 3. Numerical Formulation of Multiphase Flow in the Fractional Flow Approach

The pressure equation was solved using the standard Galerkin finite element method to obtain the total pressure at every node. Similarly, the total velocity distribution was solved by the finite element method using the calculated total pressure at each node. The upstream finite element method was used to solve two saturation equations 12 and 13. The two saturation equations were discretized as follows.

$$[C_1]\left\{\frac{\partial S_1}{\partial t}\right\}+[ADW_1]\{S_1\}+[ADT_1]\{S_t\}+[DD_1]\{S_1\}+[E_1]\{S_t\}=\{f_1\} \tag{31}$$

$$[C_2]\left\{\frac{\partial S_t}{\partial t}\right\}+[ADW_2]\{S_1\}+[ADT_2]\{S_t\}+[DD_2]\{S_1\}+[E_2]\{S_t\}=\{f_2\} \tag{32}$$

where

$$[C_1]_{i,j}=[C_2]_{i,j}=\int_\Omega \phi N_i N_j dR \tag{33}$$

$$[ADW_1]_{i,j}=\int_\Omega W_i \frac{d\kappa_1}{dS_1}\vec{V}_t \bullet \nabla N_j dR - \int_\Omega W_i \frac{d(\kappa_1 \kappa g(\rho_1-\bar{\rho}))}{dS_1}\nabla z \bullet \nabla N_j dR \tag{34}$$

$$[ADW_2]_{i,j}=\int_\Omega W_i \frac{d(\kappa_3 \kappa(\rho_3-\bar{\rho})g)}{dS_1}\nabla z \bullet \nabla N_j dR \tag{35}$$

$$[ADT_1]_{i,j}=-\int_\Omega W_i \frac{d(\kappa_1 \kappa g(\rho_1-\bar{\rho}))}{dS_t}\nabla z \bullet \nabla N_j dR \tag{36}$$

$$[ADT_2]_{i,j}=-\int_\Omega W_i \frac{d\kappa_3}{dS_t}\vec{V}_t \bullet \nabla N_j dR + \int_\Omega W_i \frac{d(\kappa_3 \kappa(\rho_3-\bar{\rho})g)}{dS_t}\nabla z \bullet \nabla N_j dR \tag{37}$$

$$[DD_1]_{i,j}=\int_\Omega \kappa_1 \kappa(1-\kappa_1)\frac{dP_{c12}}{dS_1}\nabla N_i \bullet \nabla N_j dR \tag{38}$$

$$[DD_2]_{i,j}=\int_\Omega \kappa_3 \kappa \kappa_1 \frac{dP_{c12}}{dS_1}\nabla N_i \bullet \nabla N_j dR \tag{39}$$

$$[E_1]_{i,j}=\int_\Omega \kappa_1 \kappa \kappa_3 \frac{dP_{c23}}{dS_t}\nabla N_i \bullet \nabla N_j dR \tag{40}$$

$$[E_2]_{i,j}=\int_\Omega \kappa_3 \kappa(1-\kappa_3)\frac{dP_{c23}}{dS_t}\nabla N_i \bullet \nabla N_j dR \tag{41}$$

$$\{f_1\}_i=\int_B N_i \kappa_1 V_t \bullet \hat{n} dB - \int_B N_i V_1 \bullet \hat{n} dB - \int_B N_i \kappa_1 \kappa(\rho_1-\bar{\rho})g\nabla z \bullet \hat{n} dB \tag{42}$$

$$\{f_2\}_i=\int_B N_i V_3 \bullet \hat{n} dB - \int_B N_i \kappa_3 V_t \bullet \hat{n} dB + \int_B N_i \kappa_3 \kappa(\rho_3-\bar{\rho})g\nabla z \bullet \hat{n} dB \tag{43}$$

where $W_i$ is the weighting function, $N_i$ is the Galerkin interpolation function, B indicates the boundary. Finally, if discretized Equations (31) and (32) are assembled, a simultaneous solution set is obtained in Equation (44).

$$\begin{bmatrix} C_1 & 0 \\ 0 & C_2 \end{bmatrix}\begin{Bmatrix} \frac{\partial S_1}{\partial t} \\ \frac{\partial S_t}{\partial t} \end{Bmatrix}+\begin{bmatrix} DD_1+ADW_1 \\ DD_2+\mathrm{ADW}_2 \end{bmatrix}$$
$$\begin{bmatrix} \mathrm{E}_1+ADT_1 \\ \mathrm{E}_2+ADT_2 \end{bmatrix}\begin{Bmatrix} S_1 \\ S_t \end{Bmatrix}=\begin{Bmatrix} f_1 \\ f_2 \end{Bmatrix} \tag{44}$$

The various solvers, such as Bi-CGSTAB method, modified incomplete Cholesky method, direct Gaussian elimination method, and pointwise iterative solvers, were used to obtain a simultaneous solution of the saturation equations.

## 4. Verification

Two examples have been presented to test the developed model, MPS (Suk and Yeh, 2008). The first concerned a water infiltration problem in physically and chemically homogeneous water-wet soil media. The test was performed by comparing the CHEMPS solutions with 2DFATMIC (Yeh *et al.*, 1997). The second example considered a simulation of two-phase flow of NAPL and water in the absence of gravity. In this example, the model verification was carried out by a comparison with the analytical solution reported by McWhorter and Sunada (1990). Since CHEMPS was developed based on MPS, the simulation result of CHEMPS for verification would be the same as before. Accordingly it will not be shown here.

## 5. Results and Discussions

Three different simulations are performed to illustrate the capability of CHEMPS. The first example simulates water and NAPL saturations when two circulation wells are installed in a water-NAPL system. In the second and third examples, the infiltration of a DNAPL in fully water-saturated porous media was simulated to examine the effect of physically heterogeneous and chemically heterogeneous media, respectively.

### 5.1. Two Circulation Wells in a Water-NAPL System

This example simulates water and NAPL saturations when two circulation wells are installed in a water-NAPL system. One is a water-injection well with an injection rate of 0.25 $m^3$/day, and the other is a pumping well with a total rate of 250 $m^3$/day. The location of injection and pumping wells is shown in Fig. 1. At the pumping well, depression of total pressure distribution is observed in Fig. 2 since pumping is much greater than injection. Also, water saturation has a peak at the injection well and NAPL saturation is vice-versa with water saturation as shown in Fig. 3. As expected, water flows from injection well to pumping well.

### 5.2. DNAPL Flow in Physically Heterogeneous Media

It was assumed that a low permeable lens is placed in the interior of the simulation region to examine the capillary pressure effects on DNAPL flow. The capillary pressure relations after van Genuchten model (Parker *et al.*, 1987) with the different pore size distribution index were assumed in the lens and surrounding matrix. The bottom of the reservoir was impermeable for all three phases. The hydrostatic pressure distribution for water pressure and the atmospheric pressure for the gas phase were prescribed at the left and right boundaries,

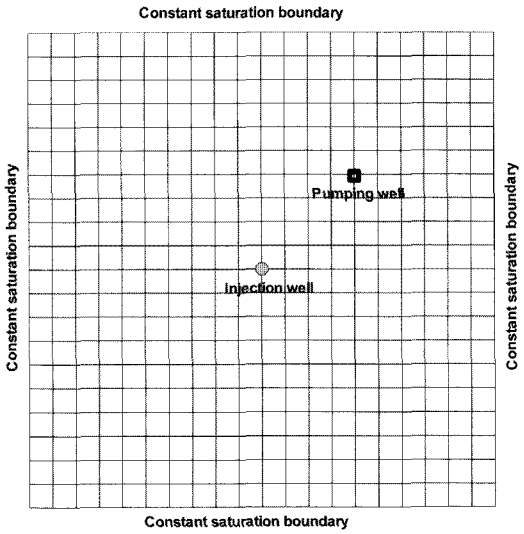


**Fig. 1.** Illustration of well locations.

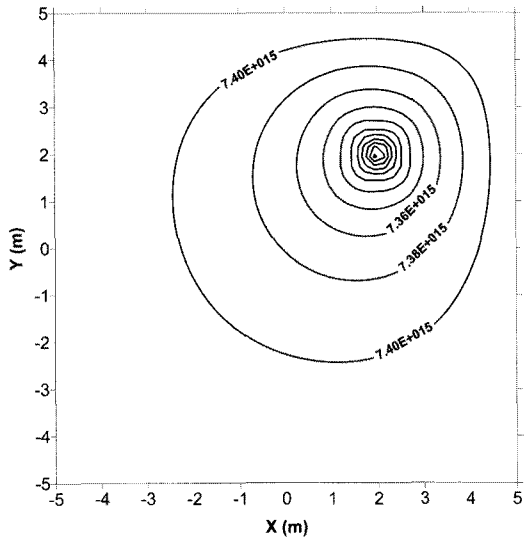


**Fig. 2.** Distribution of total pressure (g/cm/day$^2$) in the two circulation wells' problem.

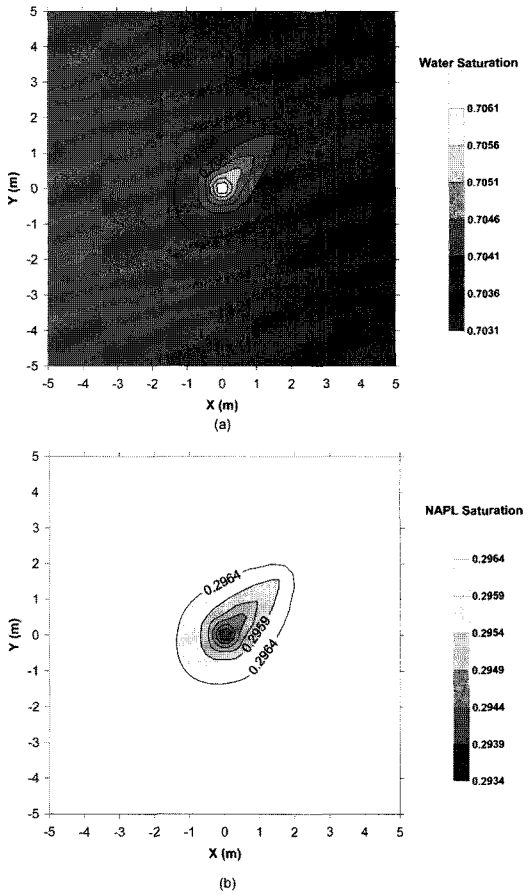


**Fig. 3.** Distribution of (a) water and (b) NAPL saturations in the two circulation wells' problem.

while for the NAPL phase, the pressure was prescribed such that the NAPL saturation is zero based on the van Genuchten model (Parker *et al.*, 1987). In other words, the pressure for the NAPL phase was equal to the air pressure. Therefore, a type 5 boundary condition was imposed on the left and right boundaries. At the inlet on the top

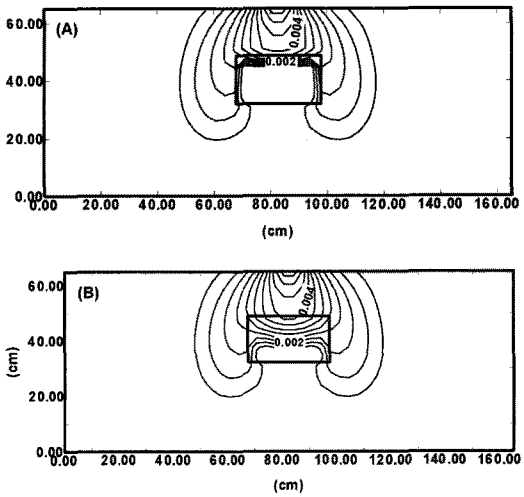


**Fig. 4.** NAPL saturation contours obtained assuming fine sand lens with the two different van Genuchten parameters, (A) n=2.80, (B) n=1.80, in the surrounding matrix (Suk and Yeh, 2008).

boundary, a flux of 10.0 cm/day for the nonwetting phase was prescribed, whereas no flow condition was prescribed for the water and air phase (Boundary Condition Type 1 in Table 2). On the remainder of the top boundary, no flux condition was imposed for all three phases. The initial conditions were as follows: hydrostatic pressure distribution for water, atmospheric condition for the gas phase, and zero saturation for NAPL (Initial Condition Type 3 in Table 1). The fluid parameters were $\rho_1$=1.00 g/cm$^3$, $\rho_2$=1.63 g/cm$^3$, $\rho_3$=1.2×10$^{-3}$ g/cm$^3$, $\mu_1$=864.0 g/cm/day, $\mu_2$=860.6 g/cm/day, and $\mu_3$=15.228 g/cm/day. The relative permeability and capillary pressure were defined from the model reported by van Genuchten (Parker *et al.*, 1987). Two different van Genuchten parameters $n$ for the lens were assumed to examine the effect of the capillary barrier on DNAPL flow for cases A and B. Table 3 lists the soil properties

**Table 3.** Soil properties for cases A and B

| Parameters | Case A | | Case B | |
|---|---|---|---|---|
| | Matrix | Lens | Matrix | Lens |
| k (cm$^2$) | 6.64×10$^{-6}$ | 3.32×10$^{-8}$ | 6.64×10$^{-6}$ | 3.32×10$^{-8}$ |
| $\phi$ | 0.43 | 0.36 | 0.43 | 0.36 |
| $\alpha_{21}$ (cm$^{-1}$) | 0.009 | 0.009 | 0.009 | 0.009 |
| $\alpha_{32}$ (cm$^{-1}$) | 0.0105 | 0.0105 | 0.0105 | 0.0105 |
| $\alpha_{31}$ (cm$^{-1}$) | 0.005 | 0.005 | 0.005 | 0.005 |
| n (van Genuchten Fitting parameter) | 2.80 | 2.80 | 2.80 | 1.80 |

for cases A and B. Figure 4A and 4B show the simulation results for case A with high $n$ and for case B with low n, respectively. A low $n$ value indicates wide pore size distribution, which reduces the entry pressure of the nonwetting phase. This means that infiltration in the lens is possible for a lower entry pressure. As shown in Fig. 4A, no DNAPL infiltrated the fine sand lens while NAPL saturation was discontinuous over the lens boundary. On the other hand, in case B, DNAPL infiltration is possible making NAPL saturation continuous throughout the lens.

### 5.3. DNAPL Flow in Chemically Heterogeneous Media

This section presents DNAPL infiltration into a physically homogeneous media with various chemical characteristics. Here, it was assumed that the chemical heterogeneities are indicated by the contact angle, which is an index of wettability, and is defined as the angle between the solid-water and water-organic contact lines. When $\theta < 90$ the water is classified as a wetting fluid, whereas the water is a nonwetting fluid at $\theta > 90$. The relationship between the capillary pressure, relative permeability, organic wet mass fraction and contact angle were defined by Bradford and Leij (1996), and Bradford *et al.* (1997, 1998). These relationships were adopted in this study. Numerical experiments were performed for four different contact angles, $\theta = 0^{\circ}$, $60^{\circ}$, $120^{\circ}$, and $180^{\circ}$ The simulation conditions were the same as those in Fig. 4A except for the homogeneous soil property and soil surface wetting characteristics. The initial and boundary conditions are the same as those given in the previous problem. As shown in Fig. 5, the depth of DNAPL infiltration decreased with increasing $\theta$ and the level of organic saturation increased. This means that the capillary pressure and relative permeability of NAPL decreases with increasing $\theta$, resulting in an decrease in the mobility of the NAPL. Therefore, the porous medium retards the NAPL more effectively.

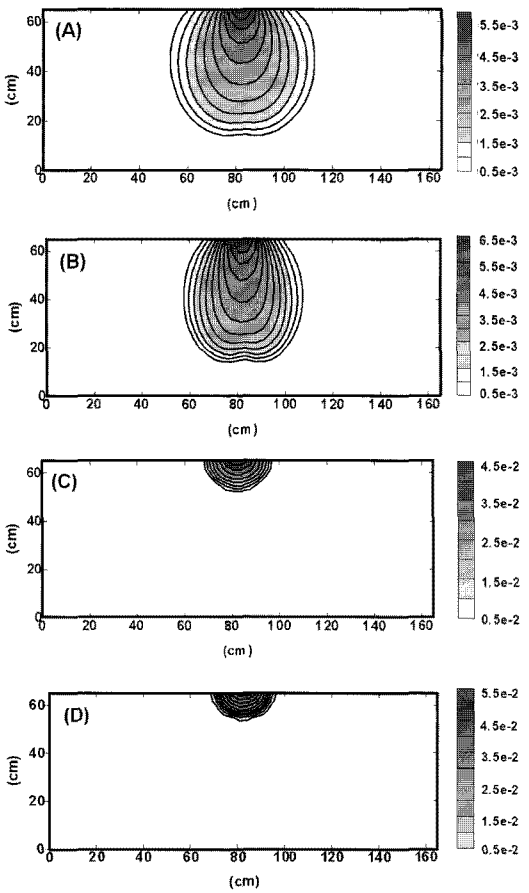


**Fig. 5.** NAPL saturation contours obtained assuming four different contact angle, (A) 0°, (B) 60°, (C) 120°, and (D) 180°.

## 6. Conclusions

This paper reports development of CHEMPS based on a fractional flow approach, which considers fully three-phase flow in physically and chemically heterogeneous media, including the mathematical and numerical formulation, numerical implementation, and a discussion of its applications. CHEMPS included the general boundary conditions, which consisted of eight combinations of two types of boundaries of individual phases, flux-type and Dirichlet-type boundaries, as well as the general initial conditions, such as eight combinations of the two types of initial condition of individual phases, saturation and pressure. In addition, this model has the ability to simulate multiphase flow under the chemically heterogeneous media as well as physically heterogeneous media.

The developed program was verified using the 2DFATMIC solutions and an exact analytical solution, which fully incorporates the effects of capillarity and relative permeability. In order to examine the effects of physically heterogeneous media on DNAPL flow, two blocks with different physically hydraulic

properties were placed in the simulation domain in the numerical experiments, whereas different contact angles were assumed in the chemically heterogeneous media. Physically heterogeneous media were characterized by the intrinsic permeability and van Genuchten parameter reflecting the pore size distribution, whereas the chemically heterogeneous media was characterized by the relationship between the contact angle, organic wet mass fraction, capillary pressure and relative permeability. In physically heterogeneous media with a wide pore size distribution, DNAPL infiltration into the low permeability lens is possible. This is because a wide pore size distribution causes a relatively lower nonwetting entry pore pressure than a narrow pore size distribution. The lower entry pore pressure can cause the DNAPL to infiltrate into a low permeability lens. In chemically heterogeneous media, the depth of DNAPL infiltration decreases with increasing contact angle and the level of organic saturation increases. This means that an increase in contact angle will result in a decrease in capillary pressure and relative permeability, which would more easily retard DNAPL flow by porous media. Overall, capillary barrier effects on organic liquid migration occur at various soil surface wetting characteristics and soil textures, due to abrupt changes in the pore size distribution.

## Acknowledgements

This subject is supported by Korea Ministry of Environment as "The GAIA project (Grant no. 173-092-009)".

## References

Bastian, P. and Helmig, R. (1999) Efficient fully-coupled solution techniques for two-phase flow in porous media parallel multigrid solution and large scale computations: *Advances in Water Resources*, v.23, p.199-216.

Binning, P. and Celia, M.A. (1999) Practical Implementation of the Fractional Flow Approach to Multi-Phase Flow Simulation: *Advances in Water Resources*, v.22, p.461-478.

Bradford, S.A., Abriola, L.M. and Leij, F.J. (1997) Wettability effects on two- and three- fluid relative permeabilities: *Journal of Contamiant Hydrology*, v.28, p.171-191.

Bradford, S.A., Abriola, L.M. and Rathfelder, K.M. (1998) Flow and entrapment of dense nonaqueous phase liquids in physically and chemically heterogeneous aquifer formations: *Advances in Water Resources*, v.22, n.2, p.117-132.

Bradford, S.A. and Leij, F.J. (1996) Predicting two- and three-fluid capillary pressure-saturation relationships of porous media with fractional wettability: *Water Resources Research*, v.32, n.2, p.251-259.

Celia, M.A. and Binning, P. (1992) Two-Phase Unsaturated Flow: One Dimensional Simulation and Air Phase Velocities: *Water Resources Research*, v.28, p.2819-2828.

Dekker, T.J. and Abriola, L.M. (2000) The influence of field-scale heterogeneity on the infiltration and entrapment of dense nonaqueous phase liquid in saturated formulations: *Journal of Contaminant Hydrology*, v.42, p.187-218.

Guarnaccia, J.F. and Pinder, G.F. (1997) *NAPL: A Mathematical Model for the Study of NAPL Contamination in Granular Soils, Equation Development and Simulator Documentation*: EPA/600/R-97/102, National Risk Management Research Laboratory, Ada, OK, 221p.

Kaluarachchi, J.J. and Parker, J.C. (1989) An Efficient Finite Elements Method for Modeling Multiphase Flow: *Water Resources Research*, v.25, p.43-54.

Kueper, B.H. and Frind, E.O. (1991a) Two-Phase Flow in Heterogeneous Porous Media, 1. Model Development: *Water Resources Research*, v.27, p.1049-1057.

Kueper, B.H. and Frind, E.O. (1991b) Two-Phase Flow in Heterogeneous Porous Media, 2. Model Application: *Water Resources Research*, v.27, p.1058-1070.

McWhorter, D.B. and Sunada, D.K. (1990) Exact Integral Solutions for Two Phase Flow: *Water Resources Research*, v.26, n.3, p.399-414.

Parker, J.C., Lenhard, R.J. and Kuppusamy, T. (1987) A Parameteric Model for Constitutive Properties Governing Multiphase Flow in Porous Media: Water Resources Research, v.23, p.618-624.

Pinder, G.F. and Abriola, L.M. (1986) On the Simulation of Nonaqueous Phase Organic Compounds in the Subsurface: *Water Resources Research*, v.22, p.109-119.

Sleep, B.E. and Sykes, J.F. (1989) Modeling the Transport of Volatile Organics in Variably Saturated Media: *Water Resources Research*, v.25, n.1, p.81-92.

Suk, H. and Yeh, G.T. (2008) Multiphase flow modeling with general boundary conditions and automatic phase-configuration changes using a fractional-flow approach: *Computational Geosciences*, v.12, n.4, p.541-571.

van der Vorst, H.A. (1992) Bi-CGSTAB: A fast and smoothly converging variant of Bi-CG for the solution of nonsymmetric kinear systems: *SIAM Journal on Scientific and Statistical Computing*, v.13, p.631-644.

van Genuchten, M. Th. (1980) A closed form equation for predicting the hydraulic conductivity of unsaturated soils: *Soil Science Society of American Journal*, v.44, p.892-898.

Yeh, G.T., Chang, J.R. and Short, T.E. (1997) 2DFATMIC: Users' Manual of a Two-Dimensional Model of Subsurface Flow, Fat and Transport of Microbes and Chemicals. EPA/600/R-97-052, National Risk Management Research Laboratory, US. EPA.

2011년 3월 11일 원고접수, 2011년 4월 22일 게재승인